NUMERICAL ANALYSIS OF NONLINEARITIES DUE TO RIGID END-STOPS IN ENERGY HARVESTERS

Sukhdeep Kaur[1], Einar Halvorsen[1], Oddvar Søråsen[2] and Eric M. Yeatman[3]
[1]Department of Micro and Nano System Technology, Vestfold University College, Norway
[2]Department of Informatics, University of Oslo, Norway
[3]Department of Electrical & Electronic Engineering, Imperial College, London

Abstract: This paper gives a numerical analysis of nonlinearities due to rigid, elastic mechanical end-stops in a vibrating energy harvester. Both an eigenvalue problem approach and time domain simulations are used. We consider two rigid end-stops limiting the motion of a proof mass. The dynamics are linear between the impacts which cause strong nonlinear behavior. Even though the output power varies little with change in acceleration amplitude, we find that there can be drastic changes in the proof mass motion with change of amplitude. In a wide range of acceleration amplitudes the phase space trajectories are very complicated and have periods much longer than the period of the vibration, some appearing chaotic. Only in a small range of amplitudes do we find simple periodic motion.

Keywords: energy harvester, nonlinearities, end-stops, impacts.

INTRODUCTION

Vibration energy harvesters are gaining popularity as a possible alternative to batteries [1]. Vibration energy harvesters can operate linearly or nonlinearly depending on device type and the amplitude of proof mass motion. Nonlinearities in the stiffness of the structure can be designed in order to improve performance [2, 3]. Nonlinearities can also appear as side effects of otherwise required design features, for example impacts of the proof mass on end-stops limiting the motion [4].

Even if the proof mass moves according to linear equations of motion between end-stops, the behaviour changes abruptly as it hits the end-stops. The non-linearity of the proof mass motion in energy harvesters that include end-stops have been studied both by simulation and experiments [3, 4].

Contrary to previous works that consider more compliant end-stops, this paper presents a numerical analysis of nonlinearities due to highly rigid, elastic mechanical end-stops in an energy harvester. The motion is treated as linear evolution between impacts with discontinuities in the velocity at the end-stops impacts. The dynamics are analyzed using both an eigenvalue problem approach and transient simulations.

MATHEMATICAL ANALYSIS

Linear equations of motion

In equilibrium, the total force on the proof mass and the voltage across the electrical load in an energy harvester must be zero. When the harvester is excited by vibrations, we will have deviations of the state variables from their equilibrium values depending on the strength of the excitation signal. The linear equations of motion of the proof mass in an energy harvester under sinusoidal excitation can be expressed with the proof mass' position x, its velocity v and the transducer charge q as state variables and with the driving force proportional to the package acceleration $a = A\cos\omega t$, where A is the peak acceleration amplitude, ω is the angular driving frequency and t is the time. For our purposes, it is more convenient to include the package acceleration and an auxiliary quantity $b = A\sin\omega t$ into the state variables to make the system autonomous. The equations of motion are then given by

$$\dot{x} = v \tag{1}$$

$$\dot{v} = -\omega_0^2 x - \frac{\omega_0^2 k}{\Gamma} q - \frac{\omega_0}{Q} v + a \tag{2}$$

$$\dot{q} = -\frac{\omega_0}{r}\Gamma k x - \frac{\omega_0}{r} q \tag{3}$$

$$\dot{a} = -\omega b \tag{4}$$

$$\dot{b} = \omega a \tag{5}$$

where, Q is the open circuit quality factor of the device, k is the electromechanical coupling factor, ω_0 is the open circuit angular resonance frequency, K is the spring stiffness, C is the transducer capacitance, $\Gamma = \sqrt{KC}$, the load resistance R is contained in $r = \omega_0 CR$ and acceleration amplitude $A = \sqrt{(a^2 + b^2)}$.

For further analysis the linear system of eq. (1) to (5) is transformed into dimensionless form. We then use a dimensionless time (phase angle) $\theta = \omega_0 t$, frequency $\varsigma = \omega / \omega_0$, amplitude $\hat{A} = A / X_s\omega_0^2$ and dimensionless state variables

$$\hat{x}(\theta) = x(t) / X_s \tag{6}$$

$$\hat{v}(\theta) = v(t) / X_s\omega_0 \tag{7}$$

$$\hat{q}(\theta) = q(t) / X_s\Gamma \tag{8}$$

$$\hat{a}(\theta) = a(t) / X_s\omega_0^2 \tag{9}$$

$$\hat{b}(\theta) = b(t) / X_s\omega_0^2 \tag{10}$$

where, $\pm X_s$ denotes the positions of the end-stops, i.e. $|x| < X_s$.

Linear evolution

With $\hat{u} = \left[\hat{x} \quad \hat{v} \quad \hat{q} \quad \hat{a} \quad \hat{b}\right]^T$ as the state vector, eq. (1) to (5) read

$$\frac{d\hat{u}}{dt} = -L\hat{u} \tag{11}$$

where,

$$\hat{L} = \begin{bmatrix} 0 & -1 & 0 & 0 & 0 \\ 1 & \frac{1}{Q} & k & -1 & 0 \\ \frac{k}{r} & 0 & \frac{1}{r} & 0 & 0 \\ 0 & 0 & 0 & 0 & \varsigma \\ 0 & 0 & 0 & -\varsigma & 0 \end{bmatrix} \tag{12}$$

Then, a linear evolution of the system from $\theta = \theta_1$ to $\theta = \theta_2$ is given by

$$\hat{u}(\theta_2) = \hat{U}(\theta_2 - \theta_1)\hat{u}(\theta_1) \tag{13}$$

where,

$$\hat{U}(\theta) = \exp(-\theta\hat{L}) \tag{14}$$

Nonlinearities at impacts

The nonlinearity due to rigid mechanical end-stops will be an abrupt change of the velocity. If we have an impact at the θ_1, this change in velocity can be modeled as $\hat{v}(\theta_1^+) = -\sqrt{e}\hat{v}(\theta_1^-)$ where e is the coefficient of restitution and the superscript +(-) denotes a time infinitesimally after (before) θ_1. For an elastic impact, e=1. Thus, the state vector change at impacts is given by

$$\hat{u}(\theta_1^+) = S\hat{u}(\theta_1^-) \tag{15}$$

where,

$$S = \begin{bmatrix} 1 & 0 & 0 & 0 & 0 \\ 0 & -\sqrt{e} & 0 & 0 & 0 \\ 0 & 0 & 1 & 0 & 0 \\ 0 & 0 & 0 & 1 & 0 \\ 0 & 0 & 0 & 0 & 1 \end{bmatrix} \tag{16}$$

Eigenvalue problem

Fig. 1 shows the end-stops model, where end-stops are placed at $\hat{x}$ =-1 and $\hat{x}$ =+1 limiting the motion of proof mass to this range. If the motion pattern (i.e. the sequence of impacts per cycle of motion) is known, all possible solutions can be found from an eigenvalue problem. Here we consider, as an example, the case where the motion is such that we get one impact on each end-stop during a cycle of motion.

Let θ =0 be the time of impact at $\hat{x} = -1$ and assume that at some intermediate time θ_1, we have another impact at $\hat{x}$ =+1 and then the next impact at $\hat{x}$ =-1 at time $\theta_2 = 2\pi/\varsigma$, thus completing one cycle of motion.

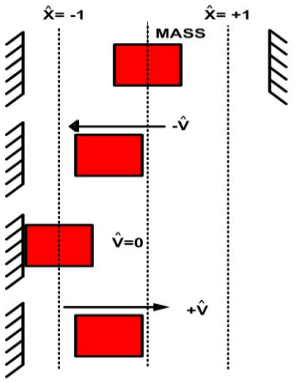

Fig. 1: Model of rigid end-stops.

If the state vector is initially $\hat{u}(0^+) = u_0$, the sequences of linear evolutions and impacts up to the time just after the second impact at $\hat{x}$ =-1 at time $\theta = \theta_2^+$ are given by

$$\hat{u}(\theta_1^-) = \hat{U}(\theta_1)u_0 \tag{17}$$

$$\hat{u}(\theta_1^+) = S\hat{u}(\theta_1^-) = S\hat{U}(\theta_1)u_0 \tag{18}$$

$$\hat{u}(\theta_2^-) = \hat{U}(\theta_2 - \theta_1)\hat{u}(\theta_1^+) = \hat{U}(\theta_2 - \theta_1)S\hat{U}(\theta_1)u_0 \tag{19}$$

$$\hat{u}(\theta_2^+) = S\hat{u}(\theta_2^-) = S\hat{U}(\theta_2 - \theta_1)S\hat{U}(\theta_1)u_0 \tag{20}$$

Now, if the period of motion is equal to the period of the vibration, we must have $\hat{u}(\theta_2^+) = u_0$ in (18). Therefore an admissible u_0 must be an eigenvector of the matrix $S\hat{U}(\theta_2 - \theta_1)S\hat{U}(\theta_1)$ with eigenvalue 1. We can therefore find candidate solutions by choosing θ_1, solving the eigenvalue problem and choosing a linear combination of eigenvectors corresponding to the eigenvalue 1 such that eq. (17) represents a real valued state vector with $\hat{x}$ =+1. The final result must be checked against unphysical solutions where the proof mass motion extends outside the limits of the end-stops. The package acceleration amplitude is then calculated from the state vectors.

It is possible to conduct similar analysis for other types of motion, but it quickly becomes complicated when there are several impacts per period of motion because that gives several unknown impact times and a new eigenvalue problem has to be formulated for each case. Therefore we also did transient simulations based on eq. (13) and eq. (15) in the following sections. This is similar to the technique used in [5].

NUMERICAL ANALYSIS

Using eq. (17) to eq. (20), MATLAB code was developed to find all possible solutions using the eigenvalue problem describing the time evolution of state vectors during one cycle of motion. For the numerical analysis, model parameters are taken from

[4] with e=1(lossless impact), r=1, ς =1(on-resonance operation), Q=350 and k^2=0.006.

The corresponding time between impacts vs. vibration (package acceleration) amplitude is shown in fig. 2. The unphysical solutions are then discarded based on a check of the displacement at intermediate times. For a normalized amplitude of 1, there is a single solution in which the first impact is at the mid-point of the cycle. As the amplitude increases this splits into two solutions with opposite asymmetry of the times between impacts.

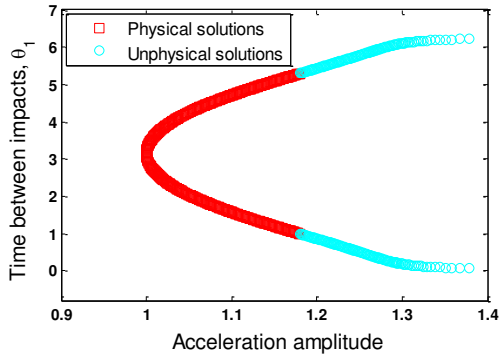

Fig. 2: Time between impacts versus acceleration amplitude.

Fig. 3 shows one cycle of motion at acceleration amplitude 1.0056 contained in the region of physical solutions in Fig. 2. The velocity discontinuities due to impact on the end-stops are evident.

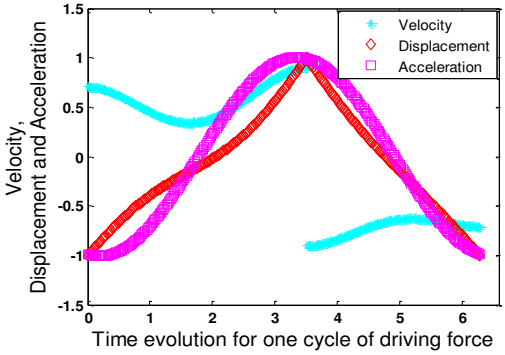

Fig. 3: Proof mass velocity $\hat{v}$ and displacement $\hat{x}$ and package acceleration $\hat{a}$ at amplitude $\hat{A}$= 1.0056.

The instantaneous output power is given by

$$\hat{P} = \frac{1}{r}\left(k\hat{x} + \hat{q}\right)^2 \qquad (21)$$

The average output power can be found by averaging eq. (19) over a period of motion. When the end-stops are not impacted, normalized average output power can be calculated from the linear model using

$$\hat{P}_{linear} = P_{linear} / mX_s^2\omega_0^3 = \frac{1}{2} r\hat{A}^2 \left|\hat{h}(\varsigma)\right|^2 \qquad (22)$$

where,

$$\hat{h}(\varsigma) = \frac{i\varsigma k}{\left\{\left(1-k^2\right) - \left(1+\frac{r}{Q}\right)\varsigma^2 + i\varsigma\left[\frac{1}{Q} + r\left(1-\varsigma^2\right)\right]\right\}} \qquad (23)$$

There exists a gap in vibration amplitudes between the range that gives linear motion and the range obtained from the eigenvalue problem described in the previous section. This gap indicates that solutions with other motion patterns must be present. In order to look into these patterns and complete the set of solutions, the system is simulated starting from an arbitrary state until the initial transients have decayed.

Fig.4 shows the average output power for the linear model, for the end-stops model calculated from the eigenvalue problem and for the system simulated for a larger numbers of vibration cycles. For the amplitude $|\hat{A}|$= 0.00658, the proof mass barely hits the end-stops. The amplitude is given by

$$\left|\hat{A}\right| = \frac{\left(r + k^2Q\right)^2 + 1}{\sqrt{\left[\left(Q^2 + r^2Q^2\right)\left(r + k^2Q\right)^2 + Q^2 + Q^2r^2\right]}} \qquad (24)$$

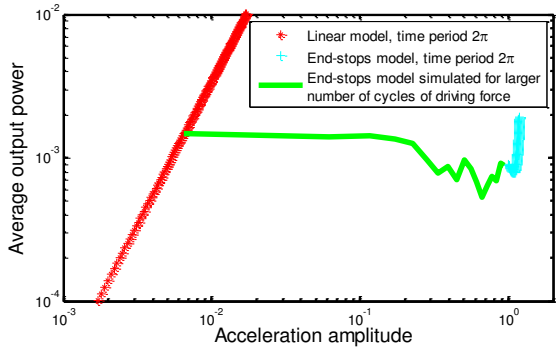

Fig. 4: Average output power versus acceleration amplitude.

In order to better understand what is happening on increasing amplitude, we have plotted phase space trajectories projected into the x-v plane in Fig. 5-8. Fig. 5 shows the time evolution for an amplitude slightly above the one that is necessary to achieve impacts. Cyclic motion is found but the period of motion is considerably longer than the period of the driving force. For slightly larger amplitude, the phase space trajectory becomes very complicated, possibly chaotic like in [6], and we are not able to observe any repeating pattern, see fig. 6.

Upon further increase of the acceleration amplitude, the motion pattern simplifies. Fig. 7 shows the phase space trajectory for $\hat{A}$=0.7. Here, periodic motion is clearly present. In this case the period is twice the period of the driving force and a stopper is hit once per period of that force. Increasing the amplitude further, we get into the range of solutions that we determined by the eigenvalue problem. Here we have the same period in the response as in the driving force and each end-stop is hit once per cycle.

We note that while the details of the motion change considerably with change in acceleration amplitude when impacts occur, the output power is only weakly dependent on the amplitude. Therefore the consequences of impacts on the performance while operating continuously are minor. Since the number of impacts per period of the driving force can change considerably with amplitude, it is an interesting

question for further investigation if the same effect is seen when the load is switched during operation. If so, it may be a challenge to utilize the end-stops as mechanical switches for power conversion circuitry. The simulation approach used in this paper can be used to analyze that situation too, provided the switching can be treated as instantaneous.

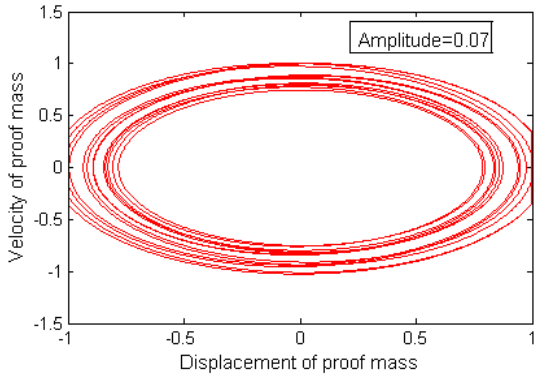

Fig. 5: Phase space trajectory in x-v plane for Â=0.07.

.

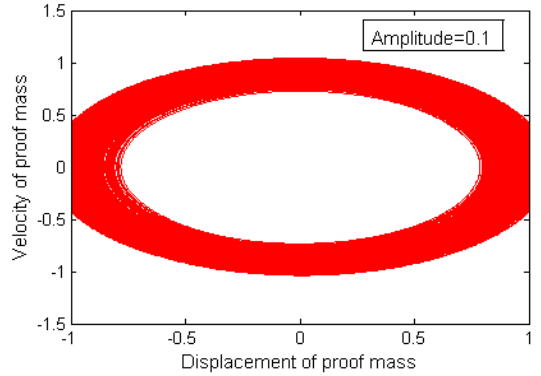

Fig. 6: Phase space trajectory in x-v plane for Â=0.10.

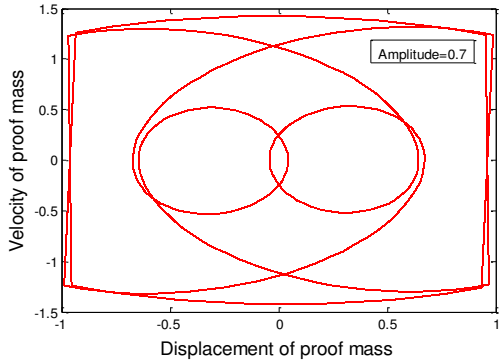

Fig. 7: Phase space trajectory in x-v plane for Â=0.70.

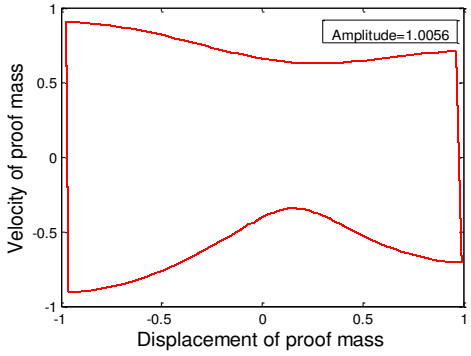

Fig. 8: Phase space trajectory in x-v plane for Â=1.0056.

CONCLUSION

A numerical analysis of impact behaviour due to rigid, elastic end-stops was presented in detail. We considered two rigid end-stops limiting the motion of the proof mass. For periodic motion with one impact on each end-stop during a period of vibration, an eigenvalue problem approach was used to study the motion of the proof mass for different amplitudes of sinusoidal excitation. It was found that this simple motion is atypical and that there are solutions with complicated trajectories in phase space. The period of motion for these solutions can be very different from the period of the driving force, if periodic at all. The main effect of end-stops on output power is to give saturation behaviour when operating in continuous mode. If the end-stops are utilized as switches for power conversion circuitry, the situation may be very different because then there has to be predictable switching on every cycle. The simulation approach used here can be used to analyse that situation and is an interesting topic for future work.

ACKNOWLEDGEMENT

This work was supported by the Research Council of Norway under Grant no. 191282.

REFERENCES

[1] Mitcheson P D, Yeatman E M, Rao G K, Holmes A S, Green T C 2008 Energy Harvesting From Human and Machine Motion for Wireless Electronic Devices Proceedings of the IEEE **96** 1457-1486.

[2] Tvedt L G W, Nguyen D S, Halvorsen E 2010 Nonlinear behaviour of an electrostatic energy harvester under wide-and narrowband excitation J. Microelecromech. Syst. **19** 305-316.

[3] Soliman M S M, Abdel-Rahman E M, El-Saadany E F, Mansour R R 2008 A Wideband vibration based energy harvester J. Micromech. Microeng. **18** 115021.

[4] Blystad L C, Halvorsen E, Husa S 2010 Piezoelectric MEMS energy harvesting systems driven by harmonic and random vibrations IEEE Transactions on Ultrasonic Ferroelectrics and Frequency Control **57** 908-919.

[5] Neubauer M, Krack M, Wallaschek J 2010 Parametric Studies on the harvested energy of piezoelectric switching techniques Smart Mater. Struct. **19** 025001.

[6] Mann B P, Owens B A 2010 Investigations of a nonlinear energy harvester with a bistable potential well Journal of Sound and Vibration **329** 1215-1226.